

Drought forecasts using data reported by the CHIRPS tool of the CHANLUD satellite weather station

Pronósticos de sequías mediante datos reportados por la herramienta CHIRPS de la estación meteorológica satelital CHANLUD

Published

Instituto Tecnológico Superior Edwards Deming, Quito - Ecuador

Periodicity

July - September
Vol. 1, Num. 26, 2025
pp. 51-69
<http://centrosuragraria.com/index.php/revista>

Dates of receipt

Received: April 02, 2025
Approved: June 11, 2025

Correspondence author

ruth_barrera@unach.edu.ec

Creative Commons License

Creative Commons License, Attribution-NonCommercial-ShareAlike 4.0 International. <https://creativecommons.org/licenses/by-nc-sa/4.0/deed.es>

Electronics and computer engineer,
National University of Chimborazo.
ruth_barrera@unach.edu.ec
<https://orcid.org/0000-0002-5656-6594>

Electronics and computer engineer,
National University of Chimborazo.
luis.tello@unach.edu.ec
<https://orcid.org/0000-0002-5274-666X>

Ruth Laura Barrera-Basantes¹
Luis Patricio Tello-Oquendo²

Abstract: The study of the characteristics and types of drought observed in recent years are indispensable elements when identifying problems related to climate change. Climatic trends accurately visualize arid and semi-arid zones, which trigger exponential changes in: crop cycles that directly affect food security, agricultural economy and the functioning of water resources infrastructures. The proposed study contributes to the construction of a stochastic model that contributes to drought forecasting in Ecuador, the technique uses information provided by the CHIRPS tool located at the CHANLUD satellite weather station, CHIRPS data were validated through statistical metrics for an ARIMA model (2,0,1). The results evidenced the presence of droughts in normal category (scarce precipitation) and extremely wet droughts (sufficient precipitation but water distribution problems), of these during the period of analysis 2000-2023 normal droughts vary between -0.99 and 0.94, corresponding to the months of January 2000 to March 2012 and April 2013 to November 2023, the extremely wet drought is between 2.38 and 4.32, for the months of April 2012 to March 2013; also the drought events did not present patterns of periodicity.

Key words: Droughts, stochastic model, ARIMA, forecasts.

Resumen: El estudio de las características y los tipos de sequía observados en los últimos años son elementos indispensables al momento de identificar problemas

relacionados al cambio climático. Las tendencias climáticas visibilizan con precisión zonas áridas y semiáridas las mismas que desencadenan cambios exponenciales en: los ciclos de cultivos que afectan directamente la seguridad alimentaria, en la economía agrícola y en el funcionamiento de infraestructuras para recursos hídricos. La propuesta de estudio contribuye a la construcción de un modelo estocástico que aporte al pronóstico de sequías en el Ecuador, la técnica utiliza información proporcionada por la herramienta CHIRPS ubicada en la estación meteorológica satelital de CHANLUD, los datos de CHIRPS se validaron a través de métricas estadísticas para un modelo ARIMA (2,0,1). Los resultados evidenciaron la presencia de sequías en categoría normal (escases de precipitaciones) y sequías extremadamente húmedas (suficientes precipitaciones pero problemas de distribución de agua), de estas durante el periodo de análisis 2000-2023 las sequías normales varían entre -0.99 y 0.94, correspondiendo a los meses de enero 2000 hasta marzo de 2012 y abril 2013 a noviembre 2023, la sequía extremadamente húmeda esta entre 2,38 y 4,32, para los meses de abril 2012 a marzo de 2013; además los eventos de sequías no presentaron patrones de periodicidad.

Palabras clave: Sequías, modelo estocástico, ARIMA, pronósticos.

Introduction

The climatological and meteorological changes of the last decades report serious problems in moorlands and water demarcations, especially in the national territory where there are 31 hydrological systems formed by 79 basins coming from watersheds that drain towards the Pacific Ocean (Patiño et al., 2023). Among the significant triggers are the impact on agricultural production, migration of human communities and reduction of structural spaces associated with industry, manufacturing and, in the last annual period, the massive impact was on the production of electricity. According to the National

Electricity Operator CENACE, it was impossible to provide Ecuadorian homes with electricity since the water reservoirs reached their minimum levels, the damage reached all fields from education, economy, technology to social coexistence itself, all thanks to the fact that the dry season or drought in the eastern basin began earlier than planned (Primicias, 2024).

Researchers such as Espín and Soria (2021) characterized the information of Andean ecosystems as the presence of a pattern of increased temperature and evapotranspiration, conditioning factors for the presence or absence of a drought. However, the World Meteorological Organization (2017) highlighted that the evolution of drought in Ecuador is complex when considering the existing relationship between El Niño Southern Oscillation (ENSO) and the spatio-temporal variability of droughts in the territory.

With the aforementioned background, several analyses have shown that the trend of droughts in the country triggers a constant risk due to the fact that the cyclicity standards of the hydrological phenomenon constantly go from a moderate category to a high category. At the same time, researcher Vergara (2023) presented reports on behalf of the United Nations Convention to Combat Drought where it was estimated that about 29% of Ecuador has experienced some degree of "significant" degradation due to the impact of droughts.

In this context, the Ministry of Environment, Water and Ecological Transition of Ecuador in June 2021 drafted the National Drought Plan in order to propose and formulate territorial strategies related to the phenomenon of drought in areas with high levels of susceptibility. Considering the background information provided, the losses related to the decrease or lack of precipitation amounted to approximately US\$424 million. The effects generated by natural phenomena are not only caused by the absence of precipitation but also by an excessive increase in precipitation (Ministry of the Environment, Water and Ecological Transition, 2021).

Regarding the monitoring of the phenomenon, the country has recorded measurements of climatological variables in a conventional manner, capturing observations from ground stations that, although accurate in regions located at high altitudes, have limitations due to limited coverage and representativeness. Spatial interpolation could become a solution; however, its usefulness generates uncertainty in places where measurement stations are dispersed (Mena et al., 2021).

This is why the proposed prediction model allows the development of mitigation and adaptation strategies to generate a contribution in the water sector, especially in vulnerable regions. The contribution to biodiversity is unavoidable since it is possible to control the alteration of ecosystems and reduce the impact on species. From the technological perspective, the advance of remote sensing highlights its capacity to offer satellite precipitation estimates with great coverage, high resolution and public accessibility after monitoring droughts, floods and landslides worldwide. This is intended to highlight the effectiveness of Climate Hazards Group Infrared Precipitation with Station (CHIRPS), a long-term satellite precipitation product designed for drought monitoring using the Standardized Precipitation Index (SPI) as an indicator of multiple droughts and space-time accuracy in terms of the geographic area of droughts.

Methodology

The design of the study was experimental considering the data collection process that used as a technique the satellite observation and conversion of raster files captured at the CHANLUD meteorological station into numerical information. The quantitative methodology allowed the construction of the standardized precipitation index (SPI) and the proposal of prediction models related to the manipulation of time series. With respect to the depth of the object of study, it was descriptive since the findings allowed characterizing the level of severity of drought and comparing it with previous studies; in terms of time, it was a cross-sectional study by monitoring the variable in the period 2000 - 2023.

Collective

The study population consisted of satellite precipitation reports taken from the CHANLUD meteorological station located in the Machángara River micro-basin for the period January 2000 to December 2023.

Data Collection Techniques and Instruments

The research used the observation technique and the collection instrument was the CHIRPS digital log downloaded from the CHANLUD weather station; the CHIRPS precipitation satellite product information combines satellite measurements and

meteorological data provided on the ground for the generation of accurate precipitation estimates. The CHIRPS product used "smart" interpolation techniques to estimate high-resolution precipitation based on infrared observations over a long-term period.

The downloaded data corresponded to daily precipitation stored in .TIF extension raster files, the necessary elements for data extraction were knowledge of the exact coordinates of the weather station focal points to ensure reporting accuracy.

Data Processing and Interpretation Techniques

Data processing used methodologies such as descriptive statistics, precipitation indicator calculation and stochastic prediction models to characterize and predict information on precipitation values that determine the presence of droughts under the following detail:

a. Descriptive Statistics

The univariate description of the climatological variable "precipitation" used libraries such as library(dplyr), library(lubridate), library(xts), library(ggplot2), library(ggpubr), library(ggh4x), library(janitor), library(SPEI), library(SEI) and library(ggpubr), by calculating numerical indicators (measures of central tendency, dispersion and shape). In addition, graphical representations such as box plots and oscillation plots that referred the behavior of the feature on a timeline were performed.

b. Determination of the Standard Precipitation Index (SPI)

The calculation and weighting of the SPI used libraries such as SPEI from the satellite station reports, the back-up methodology was the one proposed by (Edwards & McKee, 1997).

Table1 . Standardized Precipitation Index (SPI) Values

Drought Category or Severity	SPI Value
Extremely Wet	≥ 2.0
Very Wet	1.5 a 1.99
Moderately Humid	1.0 a 1.49
Normal or approximately normal	-0.99 a 0.99
Moderately dry	-1.0 a -1.49

Severely dry	-1.5 a -1.99
Extremely dry	≤ -2

Source: (Edwards & McKee, 1997).

c. Stochastic prediction model

A model is defined as autoregressive where the response variable of a period t is explained by the observations of itself in previous periods plus an error term; in addition all Y_t can be expressed as a linear combination of its historical values in the same way plus the error. Autoregressive models are represented by the word AR which indicates the order of the model: AR (1), AR (2),...etc. The order of the model expresses the number of lagged observations of the analyzed time series. Thus, for example, an AR (1) model would have the expression shown in equation 1:

$$Y_t = \phi_0 + \phi_1 Y_{t-1} + a_t$$

The error term of models of this type is generally called white noise when it meets the three traditional basic assumptions: zero mean, constant variance and zero covariance between errors corresponding to different observations. The generic expression of an autoregressive AR(p) model would be as shown below:

$$Y_t = \phi_0 + \phi_1 Y_{t-1} + \phi_2 Y_{t-2} + \dots + \phi_p Y_{t-p} + a_t$$

In abbreviated form the model would be:

$$\phi_p(L)Y_t = \phi_0 + a_t$$

Where $\phi_p(L)$ is known as the polynomial lag operator and where, in turn, the term L is known as the lag operator such that, applied to the value of a variable at t, results in the value of the same variable at t-1.

$$(L)Y_t = Y_{t-1}$$

If the process is replicated successively p times it delays the value in p periods as referred to in the equation:

$$(L)^p Y_t = Y_{t-p}$$

Data processing was performed in R programming language, for organization of tables and other second order results an Excel spreadsheet was used.

Results

Descriptive Statistics

The following information corresponds to the univariate description of the precipitation variable from the reports of the CHANLUD satellite meteorological station; at this stage of the study, numerical indicators and comparative graphs were used throughout the years.

Table 2. Numerical indicators of "Precipitation" period 2000-2023

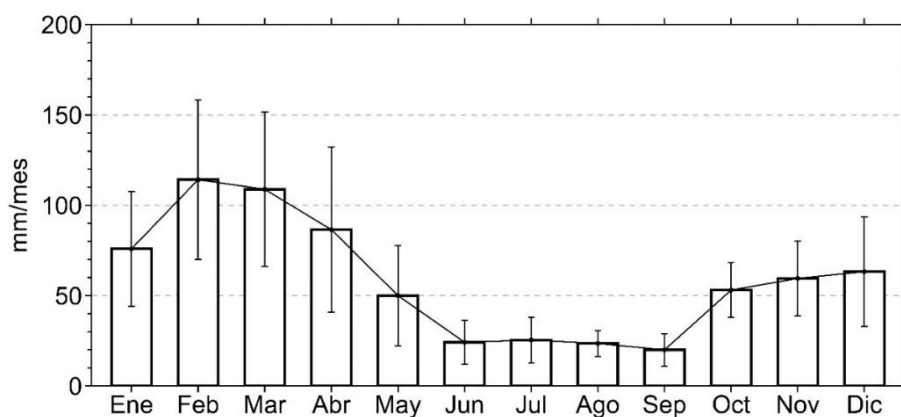
Precipitation Indicators	
Average	61,42
Standard error	3,30
Median	47,56
Mode	amodal
Standard deviation	75,03
Sample variance	5629,77
Kurtosis	92,32
Skewness coefficient	8,26
Range	981,88
Minimum	9,8
Maximum	991,68

Source: Authors.

The report of 23 years showed that the annual rainfall was 61.42 ml/m² variation was 75.03 ml/m², the kurtosis value of 92.32 reflected the presence of a leptokurtic distribution or in turn, in reinforcement to the above mentioned, the maximum value of 991.68 ml/m² represented the presence of very intense rains during the interval. Likewise, the minimum value of 9.8 ml/m² reflected the minimum presence of rainfall, the extremes of the variable evidenced both the presence of extremely strong storms and the presence of droughts, which reveals a disorderly climatic change related to an unusual climatic pattern.

The following multiple plots show the comparative trend of precipitation at the satellite level.

Figure 1. Monthly interannual comparison between 2000 and 2023 satellite stations.



Source: Author

The behavior of the satellite information lacks a defined trend, the time series that collects the interannual monthly values of the 23 years reflected a variation in the cyclicity over time, an inescapable unimodal distribution was reported where the months with the highest precipitation were February and with a minimal difference March; those with the lowest precipitation were June, July, August and September. Jiménez et al. (2024) validated the findings constructed from satellite data due to characteristics such as a wider coverage when monitoring large areas that are difficult to access for ground stations. In relation to technology, satellites, thanks to radars and infrared sensors, detect humidity levels and rainfall intensity with greater precision.

On the other hand, Perez et al., (2020) in a climate trend study period 1976 to 2017 determined that according to the multi-year monthly averages there was a dry climate in the months of June to September and a wet climate in two intervals (February - May and October - December). (2004) in the South American Amazon determined that the wave analysis of the Amazonian hydrological regime shows a high temporal instability with intermittent interannual and interdecadal oscillations during the years 1903-1998; therefore, on interannual

scales, precipitation can be high and low and these changes can be associated with the El Niño phenomenon.

In contrast to these results, Oñate and Bosque (2001) reported that in the southern zone of Ecuador and northern Peru, a report of 40 meteorological stations from 1970 to 2000 showed decreasing trends in the highlands and increasing trends in the lowlands, a contribution that was not taken into account by the authorities in charge of hydroelectric plants after warning of a significant decrease in precipitation and a possible increase in extreme events.

Table 3. *Statistical metrics of the satellite report*

Metric	Value
Relative bias	0.52
Pearson correlation	0.75
Root mean square error (RMSE)	65.23
Fractional RMSE	0.39

Source: Author

The relative bias allowed validating the precision and accuracy of the reports, a value of 0.52 revealed that the estimator overestimated the true precipitation value, which evidenced the lack of quality control processes of the equipment used for data collection. With respect to the mean square error, notable discrepancies were observed between the possible predictions and their real value, which suggests the use of time series tools that do not involve the association between two characteristics, but work with their own outdated information. The RMSE indicator may detract from the modeling if one considers the information of its variant Fractional RMSE indicator which indicated that the average model error is approximately 39%.

Standardized Precipitation Index (SPI) Construction

The SPI was constructed under the SPEI functions package whose transformation of the variable was in monthly periods, then its results were discretized through a frequency distribution to identify the category of droughts that could be of different nature according to the categories proposed in Table 1 of the document.

Table 4. Standardized precipitation index classification

Category or severity of drought	Frequency	Percentage
Extremely wet	16	5,6
Moderately Humid	1	0,3
Moderately Dry	1	0,3
Normal	270	93,8
Total	288	100

Source: Author

93.8% of the SPI ruled out the absence of droughts since according to the indicator the precipitation described a normal climatic behavior, 5.6% were extremely humid droughts, only 0.3% was the percentage of representativeness for the moderately humid and moderately dry categories.

Stochastic model for the standardized precipitation index SPI

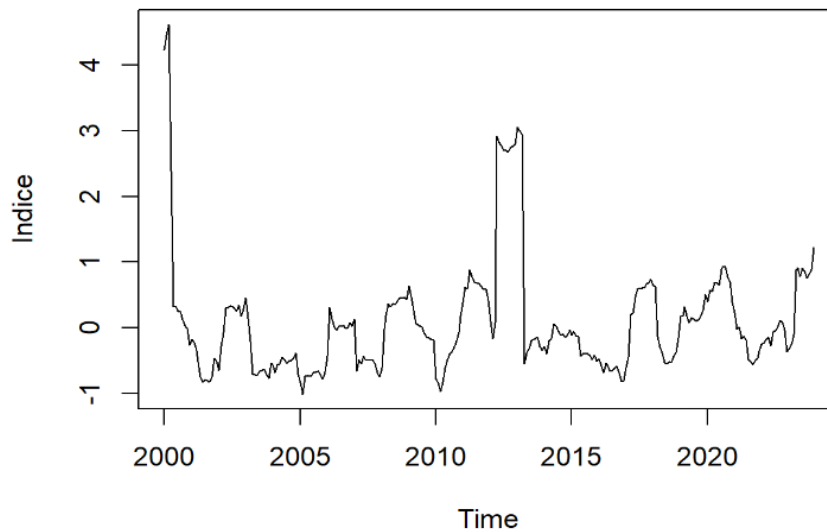
For the construction of the stochastic model, the indexes were organized in a numerical vector of information that represented the standardization of each of the precipitation values in the 23 years of historical analysis.

Figure 2 . SPI time series period 2000-2023.

	Jan	Feb	Mar	Apr	May	Jun	Jul	Aug	Sep	Oct	Nov	Dec
2000	4.24	4.46	4.62	2.39	0.32	0.33	0.26	0.24	0.12	0.04	-0.01	-0.26
2001	-0.18	-0.22	-0.34	-0.52	-0.75	-0.82	-0.79	-0.80	-0.83	-0.75	-0.46	-0.51
2002	-0.65	-0.29	-0.08	0.30	0.31	0.33	0.32	0.30	0.26	0.34	0.18	0.29
2003	0.45	0.14	-0.21	-0.70	-0.72	-0.73	-0.66	-0.65	-0.63	-0.72	-0.77	-0.54
2004	-0.56	-0.68	-0.56	-0.55	-0.45	-0.48	-0.54	-0.51	-0.50	-0.46	-0.38	-0.70
2005	-0.84	-1.01	-0.74	-0.73	-0.74	-0.73	-0.68	-0.67	-0.66	-0.72	-0.78	-0.67
2006	-0.43	0.31	0.13	0.01	-0.03	0.02	0.02	0.03	-0.01	-0.01	0.08	0.02
2007	0.13	-0.66	-0.48	-0.55	-0.43	-0.49	-0.50	-0.49	-0.48	-0.55	-0.68	-0.75
2008	-0.61	-0.02	0.19	0.36	0.32	0.37	0.35	0.41	0.45	0.45	0.46	0.43
2009	0.64	0.47	0.27	0.07	0.05	0.02	0.01	-0.09	-0.14	-0.15	-0.18	-0.19
2010	-0.78	-0.84	-0.97	-0.83	-0.60	-0.48	-0.39	-0.36	-0.28	-0.20	-0.07	0.18
2011	0.39	0.62	0.60	0.88	0.77	0.70	0.69	0.67	0.63	0.59	0.60	0.42
2012	0.10	-0.16	0.08	2.92	2.82	2.78	2.70	2.70	2.68	2.75	2.77	2.80
2013	3.06	3.00	2.94	-0.55	-0.38	-0.32	-0.20	-0.17	-0.16	-0.14	-0.28	-0.34
2014	-0.28	-0.40	-0.20	-0.16	0.06	0.04	-0.05	-0.11	-0.10	-0.14	-0.11	-0.03
2015	-0.11	-0.05	-0.13	-0.13	-0.43	-0.40	-0.39	-0.40	-0.42	-0.48	-0.42	-0.51
2016	-0.47	-0.58	-0.68	-0.54	-0.59	-0.66	-0.65	-0.62	-0.58	-0.68	-0.81	-0.80
2017	-0.60	-0.45	0.20	0.22	0.46	0.60	0.60	0.61	0.62	0.67	0.67	0.74
2018	0.65	0.63	-0.13	-0.30	-0.38	-0.53	-0.55	-0.52	-0.53	-0.43	-0.37	-0.15
2019	0.18	0.18	0.32	0.18	0.08	0.16	0.13	0.10	0.12	0.18	0.27	0.51
2020	0.40	0.58	0.55	0.70	0.69	0.65	0.89	0.94	0.93	0.77	0.71	0.39
2021	0.23	-0.02	0.01	-0.16	-0.13	-0.19	-0.48	-0.52	-0.56	-0.49	-0.46	-0.35
2022	-0.25	-0.23	-0.17	-0.14	-0.27	-0.06	-0.04	0.01	0.11	0.09	-0.03	-0.36
2023	-0.32	-0.25	-0.10	0.88	0.92	0.78	0.91	0.86	0.76	0.82	0.89	1.23

Source: Author

Figure 3. SPI time series



Source: Author

The creation of the time series graph allows evaluating the presence of stationarity in order to facilitate the analysis and modeling of the indicator and thereby ensure that statistical properties such as the mean and variance are constant over time. The visual report appeared that the SPI values are stationary; however, the Dickey Fuller test at 5% significance was used under the following hypotheses:

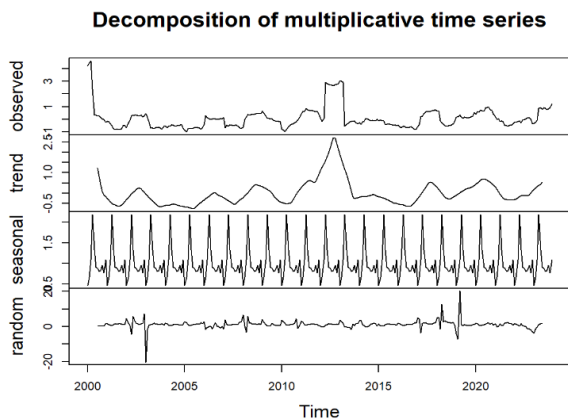
H0: The time series is not stationary.

H1: The time series is stationary.

The probability value was 0.01 which verified compliance with stationarity ($p\text{-value} \leq \alpha$: Reject H0).

Additionally to evaluate the characteristics of the time series.

Figure 4. SPI time series characteristics.

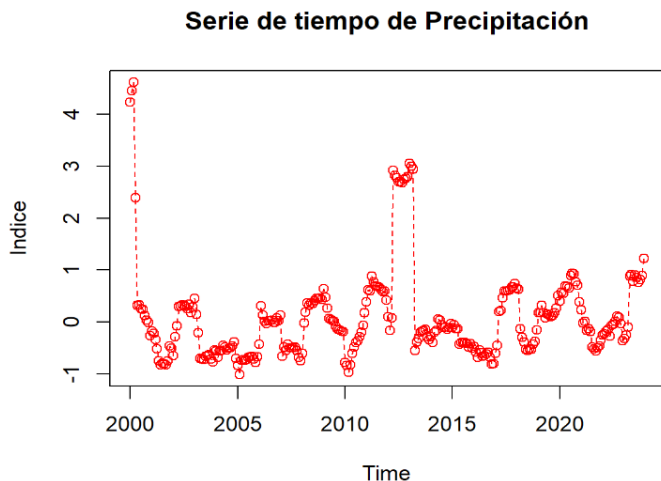


Source: Author

The composite plot demonstrated the presence of a constant long-term trend, the seasonality evidenced the fulfillment of monthly patterns in terms of constant increase or decrease of precipitation, the random component (noise) guaranteed the variability of the data.

Figure 5 shows the base series for the construction of the model.

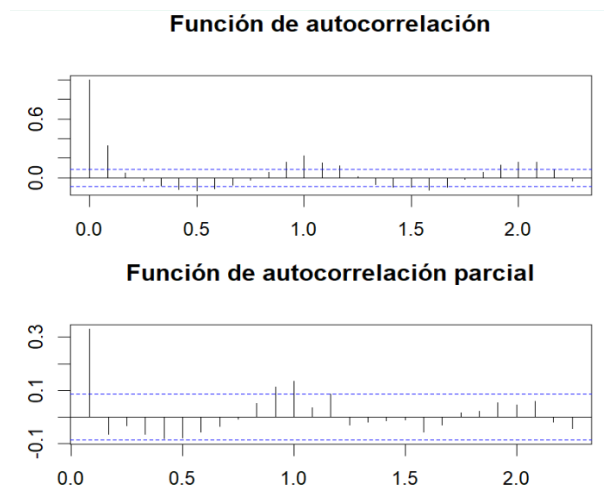
Figure 5. SPI stationary time series.



Source: Author

To define the model parameters, the autocorrelation function and the partial autocorrelation function were calculated in order to define the number of autoregressives and moving averages used in the ARIMA model.

Figure 6. Autocorrelation function and partial autocorrelation function of the SPI.



Source: Author

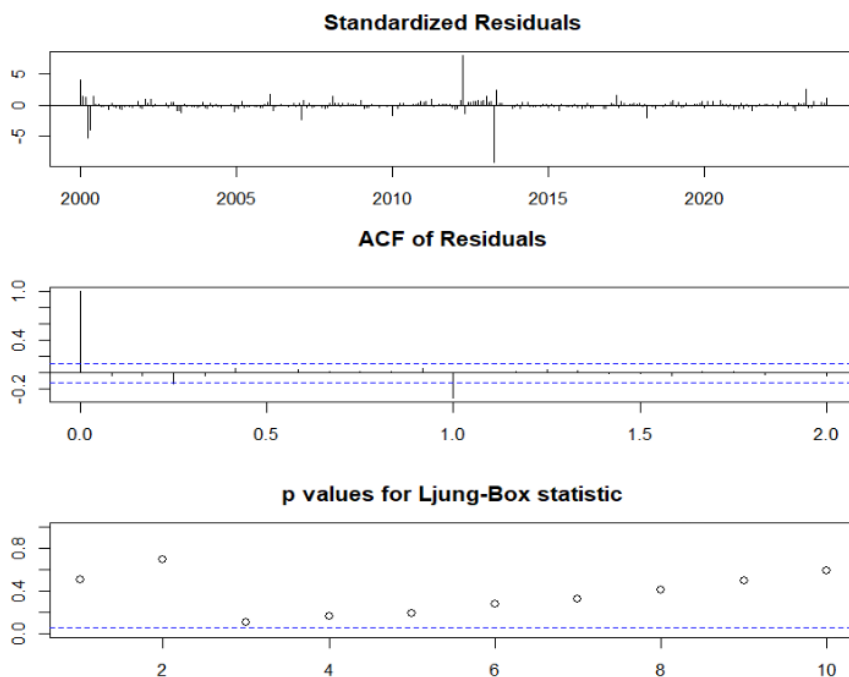
According to the graphical report of the ACF and PACF functions, the proposed model used 2 autoregressive, zero differences because the series was stationary from its origin file and an ARIMA moving average (2,0,1), each of the parameters are shown in Figure 6.

The model under the parameters would be according to the equation

$$Y_t = 0.224 + 1,25a_{t-1} - 0,33a_{t-2} + e_i$$

For the validation of the model, the diagnostic graph was constructed in order to evaluate the presence of white noise and guarantee the prediction of standardized precipitation index values in the coming years.

Figure 7. Characteristics of the SPI ARIMA (2,0,1) model.



Source: Author

Although the graph showed the presence of white noise, the Ljung Box inferential test was performed at 5% significance under the following hypotheses:

H0: There is white noise in the SPI series.

H1: There is no white noise in the SPI series.

The probability value was 0.05 which verified the presence of white noise in the series ($p\text{-value} \leq \alpha$: Reject H0), this validates the constant variance, mean equal to zero and the absence of correlations to handle data independence.

Calculation of forecasts

Figure 8. Model forecasts

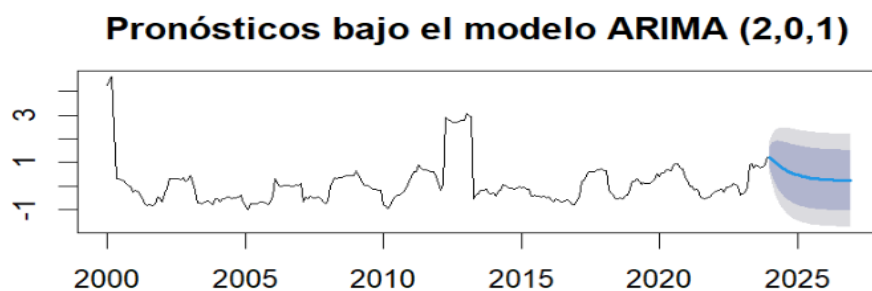
	Point Forecast	Lo 80	Hi 80	Lo 95	Hi 95
Jan 2024	1.2184692	0.765630635	1.671308	0.52591240	1.911026
Feb 2024	1.1415712	0.459706033	1.823436	0.09874841	2.184394
Mar 2024	1.0486754	0.208309402	1.889041	-0.23655350	2.333904
Apr 2024	0.9573048	0.004526012	1.910084	-0.49984459	2.414454
May 2024	0.8731497	-0.160968063	1.907268	-0.70839696	2.454696
Jun 2024	0.7975648	-0.296420000	1.891550	-0.87554055	2.470670
Jul 2024	0.7303689	-0.408283408	1.869021	-1.01104953	2.471787
Aug 2024	0.6708861	-0.501444059	1.843216	-1.12203818	2.463810
Sep 2024	0.6183261	-0.579597403	1.816250	-1.21373981	2.450392
Oct 2024	0.5719187	-0.645569665	1.789407	-1.29006906	2.433906
Nov 2024	0.5309569	-0.701554085	1.763468	-1.35400601	2.415920
Dec 2024	0.4948069	-0.749277593	1.738891	-1.40785613	2.397470

Source: Author

The prediction model requested the construction of 12 SPI values corresponding to the year 2024, each of the forecasts presented confidence intervals at 80% and 95% of significance, the positive or negative sign of the interval limits represent the increase or decrease of the SPI index over time.

The information in the table is shown in the following value extension graph.

Figure 9. SPI time series and model forecasts



The present research used precipitation reports from the CHANLUD weather station for SPI calculation and the results found are reason for contrast with the stochastic model proposed in the research of Saquisili (2019). In that research, a stochastic model was proposed for drought prediction using climate and reanalysis data for the Machangara river sub-basin but with the difference that the precipitation values for SPI calculation were captured from the CHANLUD ground weather station.

The comparative study developed the proposal of 12 ARIMA models fitted on the time series of the standardized precipitation index with the parameters described in Figure 10.

Figure 10. ARIMA models proposed in the comparative study.

Mes	Estación	Variable de respuesta	Modelo para \hat{N}_t	Modelo para \hat{N}_t
Enero	Chanlud	SPI3	ARIMA(1,0,1)	ARIMA(1,0,5)
Febrero	Chanlud	SPI3	ARIMA(0,1,1)	ARIMA(3,0,2)
Marzo	Chanlud	SPI3	ARIMA(1,0,5)	ARIMA(0,1,2)
Abril	Chanlud	SPI3	ARIMA(2,0,5)	ARIMA(1,1,0)
Mayo	Chanlud	SPI3	ARIMA(3,1,0)	ARIMA(3,0,3)
Junio	Chanlud	SPI3	ARIMA(4,0,0)	ARIMA(3,1,0)
Julio	Chanlud	SPI3	ARIMA(0,1,1)	ARIMA(0,1,1)
Agosto	Chanlud	SPI3	ARIMA(0,1,1)	ARIMA(0,1,1)
Septiembre	Chanlud	SPI3	ARIMA(2,1,0)	ARIMA(0,1,1)
Octubre	Chanlud	SPI3	ARIMA(2,0,0)	ARIMA(3,1,0)
Noviembre	Chanlud	SPI3	ARIMA(1,1,4)	ARIMA(3,1,1)
Diciembre	Chanlud	SPI3	ARIMA(1,1,0)	ARIMA(0,1,5)

Source: (Saquisili, 2019).

Saquisili (2019) mentioned that the proposed models in most cases are not stationary which invalidates the calculation of forecasts with any of the models however the present research built an ARIMA (10,0,1) model that guaranteed stationarity and white noise. This showed that data from satellites collect more information compared to terrestrial information; on the other hand, data collection of climatic variables is more accurate in satellite information due to the location of the meteorological station.

On the other hand, the author Saquisili (2019) mentions "The SPI3 values for the analysis period 1965-2015, show that moderate, severe and extreme drought events, have taken place in the study area. For the labrado station, moderate drought varies between -1 and -1.45, corresponding to the months of December 1966 and August 1992; severe drought ranges between -1.52 and -1.96, for the month of June 2014 and December 1989; and extreme drought is between -2.02 and -2.84, for the month of August 2012 and November 2010, respectively. While, in the CHANLUD station, the moderate drought ranges between -1 and -1.48, corresponding to the months of February 1969 and August 2003; the severe drought fluctuates between -1.51 and -1.78, recorded in the month of October 2001 and May 1967, respectively; and the minimum extreme drought is recorded in April 2013 with a value of -2 and the maximum is recorded in December 2000, with a value of -3.08. All drought events have a duration of 1 to

4 months. Also, it could be identified that, throughout the period of analysis, there are no drought events that show a certain periodicity".

In this research, the SPI for the period of analysis 1981-2023, identifies normal, moderately dry and extremely wet drought events. The normal droughts vary between -0.99 and 0.94, corresponding to the months from January to December from 1981 to 2023 with a total of 422 months of the 516 months observed in the 42 years; the moderately dry drought ranges between -1.00 and -1.47, for the months of April, June August, November and December of the years 1982, 1985, 1986, 1987, 1988, 1989, 1990, 1991 and 2005; and extremely wet drought is between 2.38 and 4.32, for the months of August to December 1999, January to April in 2000, April to December 2012 and January to March 2013. The drought events did not show patterns of periodicity.

Conclusions

The usefulness of the CHIRPS tool guarantees reliability in the climate data collected thanks to an almost global coverage since 1981 with a resolution of 0.05° between 50°S and 50°N , its information matrix stores precipitation values from satellite estimates of great value and these were validated through metrics such as Pearson Correlation Index, Relative Bias, Pearson Correlation, Root Mean Square Error (RMSE) and Fractional RMSE.

The Standardized Precipitation Index (SPI) indicates, according to its percentage distribution, that 93.8% of the values of the indicator denote the presence of droughts with normal behavior and 5.6% correspond to extremely wet droughts.

With reference to the SPI values during the observation period 2000-2023, there were normal and extremely humid drought events. Normal droughts vary between -0.99 and 0.94, these appeared in the months of January 2000 to March 2012 in a continuous monthly basis and then reappeared in April 2013 to November 2023; this means that during the indicated months Ecuador presents a shortage of rainfall so that the natural climatic condition negatively affects water resources, agriculture and the environment. On the other hand, the extremely humid drought is between 2.38 and 4.32, it was present in the months of April 2012 to March 2013; which indicates that despite having sufficient rainfall in general terms, there are problems of water

shortage due to factors such as uneven distribution of rainfall, poor water management or lack of adequate infrastructure.

References

- ACCOTECNIC (2022). Machangara river sub-basin.
- Acevedo, S., Mrkaic, M., Novta, N., and Pugacheva, E. (2018). The effects of weather shocks on economic activity: what are the channels of the impact?
- Bocco, G., Orozco, Q., Alvarez, A., Solis, B., and Dobler, C. (2021). Studying the impact of drought in small rural communities in Mexico: a review of the literature. *Bibliographical Journal of Geography and Social Sciences*, 26(1314).
- Climate Hazard Center. (2025). CHIRPS. <https://www.chc.ucsb.edu/data/chirps>
- Cobo, J., Ortiz, I., Sánchez, J., and Ordieres, J. (2009). State of the art of competency measurement in project management.
- Gavilanes, C. (2024). Cost analysis in early warning systems using meteorological drought values through long-term satellite information of the CHIRPS product. National University of Chimborazo.
- Gutiérrez, D. (2022). What can we tell you at AEMET about drought? Agencia estatal de meteorología: <https://repositorio.aemet.es/handle/20.500.11765/14643>
- Jimenez, E., Murillo, A., and Delgado, D. (2024). Comparative analysis of precipitation databases for the province of Manabí. *Revista Científica Arbitrada Multidisciplinaria PENTACIENCIAS*, 6(1).
- Labat, D., Ronchail, J., Callede, J., Guyot, J., De Oliveira, W., and Guimaraes, E. (2004). Wavelet analysis of Amazon hydrological regime variability. *Geophysical research letters*.
- Lazo, P. (July 4, 2023). Drought challenges architecture. *Arquine*.
- Melgarejo, J., López, M., and Fernández, P. (2021). Floods and Droughts: Multidisciplinary analysis to mitigate the impact of external climatic phenomena. University of Alicante. <https://doi.org/978-84-1302-138-6>
- Mena, V., Scheffczyk, K., and Urrutia, M. (2021). Flood Risk Assessment in Ecuador.
- Ministry of Environment, Water and Ecological Transition (2021). National Drought Plan (Ministerio del Ambiente Agua y

- Transición Ecológica. <https://www.ambiente.gob.ec/wp-content/uploads/downloads/2022/01/PLAN-NACIONAL-DE-SEQUIA.pdf>
- Ministry for Ecological Transition and the Demographic Challenge (2022). Types of drought. https://www.miteco.gob.es/es/agua/temas/observatorio-nacional-de-la-sequia/que-es-la-sequia/observatorio_nacional_sequia_1_1_tipos_sequia.html
- Muñoz, P., Díaz, D., Cabrera, S., and Jácome, G. (2025). Water scarcity index in the Ambi river basin, Ecuador. *Water Technology and Science*, 16(1).
- Oñate, F., and Bosque, J. (2001). Study of climate trends and generating regional climate change scenarios in a binational river basin in South America. *Geographical studies*.
- World Meteorological Organization. (2017). Multi-hazard early warning systems: checklist.
- Patiño, N., Carrión, H., Brito, J., and Hidalgo, D. (2023). Study of the hydrological response of the Catamayo - Chira basin to extreme events (floods, droughts). *Polo del conocimiento*, 8(12).
- Pérez, N., Mullo, H., and Marcatoma, A. (2020). Analysis of climate change in a high Andean ecosystem Riobamba - Ecuador. *Profiles*, 1(23).
- Primicias (2024). Electric crisis will continue in 2024 and 2025: drought begins in August and Paute goes to maintenance. <https://www.primicias.ec/noticias/economia/crisis-electrica-cortes-luz-hidroelectrica-paute/>, 2.
- Serrano, S., Aguilar, S., Aguilar, E., Martínez, R., Hernández, M., and Azorín, C. (2017). The complex influence of ENSO on droughts in Ecuador. *Climate Dynamics*, 48.
- Vergara, V. (2023). Desertification and drought in Ecuador: consequences of climate change? *Elements Journal*(1).
- Zhiña, D., Pacheco, J., and Avilés, A. (2017). Stochastic models for drought forecasting in the Chulco River micro-watershed in Ecuador. *Journal of the Faculty of Chemical Sciences*(16).